STEM CELLS TRANSLATIONAL MEDICINE®

TISSUE ENGINEERING AND REGENERATIVE MEDICINE

Humanized Culture of Periosteal Progenitors in Allogeneic Serum Enhances Osteogenic Differentiation and In Vivo Bone Formation

SCOTT J. ROBERTS,[a,b,c,*] HELEN C. OWEN,[d,*] WAI LONG TAM,[a,b] LIEN SOLIE,[d] SOPHIE J. VAN CROMPHAUT,[d] GREET VAN DEN BERGHE,[d] FRANK P. LUYTEN[a,b]

Key Words. Adult stem cells • Bone • Culture • Differentiation • Mesenchymal stem cells • Osteoblast • Tissue regeneration

[a]Laboratory for Developmental and Stem Cell Biology, Skeletal Biology and Engineering Research Center, [b]Prometheus, Division of Skeletal Tissue Engineering, and [d]Department and Laboratory of Intensive Care Medicine, KU Leuven, Leuven, Belgium; [c]Institute of Orthopaedics and Musculoskeletal Science, Division of Surgery & Interventional Science, University College London, The Royal National Orthopaedic Hospital, Stanmore, Middlesex, United Kingdom

[*]Contributed equally as first authors.

Correspondence: Scott J. Roberts, Ph.D., Skeletal Biology and Engineering Research Center, Onderwijs en Navorsing 8th floor, bus 813, B-3000 Leuven, Belgium. Telephone: 32-16-34-61-38; E-Mail: scott.roberts@med.kuleuven.be

Received October 18, 2012; accepted for publication August 6, 2013; first published online in SCTM *Express* December 27, 2013.

http://dx.doi.org/10.5966/sctm.2012-0137

ABSTRACT

The translation of stem cell-based regenerative solutions from the laboratory to the clinic is often hindered by the culture conditions used to expand cell populations. Although fetal bovine serum (FBS) is widely used, regulatory bodies and safety concerns encourage alternative, xeno-free culturing practices. In an attempt to apply this approach to a bone-forming combination product of human periosteal progenitors (human periosteum derived cells) on a clinically used calcium phosphate carrier, FBS was substituted for human allogeneic serum (hAS) during cell expansion. It was found that cell proliferation was increased in hAS along with an apparent commitment to the osteogenic lineage, indicated by enhanced Runx2 expression, as well as alkaline phosphatase activity and matrix mineralization. Following analysis of signaling pathways, it was found that interferon-mediated signaling was downregulated, whereas JAK-STAT signaling was upregulated. STAT3 phosphorylation was enhanced in hAS-cultured human periosteum derived cells, inhibition of which ablated the proliferative effect of hAS. Furthermore, following in vivo implantation of hAS-cultured cells on NuOss scaffolds, enhanced bone formation was observed compared with FBS (71% increase, $p < .001$). Interestingly, the de novo-formed bone appeared to have a higher ratio of immature regions to mature regions, indicating that after 8 weeks implantation, tissue-formation processes were continuing. Integration of the implant with the environment appeared to be altered, with a decrease in calcium phosphate grain size and surface area, indicative of accelerated resorption. This study highlights the advantages of using humanized culture conditions for the expansion of human periosteal progenitors intended for bone regeneration. STEM CELLS TRANSLATIONAL MEDICINE *2014;3:218–228*

INTRODUCTION

Mesenchymal stem cells (MSCs) are multipotent cells capable of self-renewal and differentiation into specialized cell types including adipocytes, osteoblasts, and chondrocytes [1]. In addition, MSCs have been shown to be immunosuppressive. Because of these characteristics, they have been proposed for use as cellular therapeutics in autoimmune and immune-mediated diseases; however, following extraction from tissues such as adipose, muscle, bone marrow, or the periosteum, MSCs must be expanded ex vivo to reach sufficient numbers for cellular therapy or tissue repair applications. Consequently, culture conditions should be optimized to allow high proliferation while maintaining stemness and function. MSCs are generally expanded in media containing fetal bovine serum (FBS), which is isolated by harvesting blood from fetal calves through cardiac puncture at around 6 months of fetal development [2].

Although it allows cell attachment and sustained cell proliferation and differentiation, the use of FBS in culture conditions has been criticized because, in addition to growth factors and nutrients, FBS contains animal proteins and potential infectious agents, thereby eliciting immunological responses [2]. In particular, infectious agents such as prions, bacteria, viruses, mycoplasma, yeast, and fungi can be difficult to remove from the serum, raising concerns about the use of FBS in culture conditions for cells prior to cell therapy [3, 4]. In addition, the presence of xenogeneic proteins in FBS can alter the outcome of cell-based therapies. Anti-FBS antibodies have been reported in a clinical trial of osteogenesis imperfecta, possibly leading to graft failure [5]. These antibodies were also detected in patients who received an allogeneic transplantation of hematopoietic stem cells prior to an injection of MSCs cultured in FBS-containing media [6].

Ethical problems related to the use of FBS in cell culture conditions are yet another challenge to overcome because it has been reported that isolation of FBS from fetal calves is generally accompanied by an awareness of pain and

discomfort [7]. Although pain-minimizing techniques exist for FBS isolation, general adaptation of these techniques remains problematic [2, 8]. In addition, approximately 1 million fetal calves are killed each year for collection of around 500,000 l of FBS, conflicting with the ethical message of "reducing, replacing, and refining" animal experimentation in biomedical research [9]. Consequently, it is clear that the culture and expansion of clinical grade human MSCs (hMSCs) requires alternatives to FBS. A number of animal serum substitutes have been tested previously for their ability to sustain proliferation and differentiation of hMSCs; however, a major caveat is the incapability of hMSCs to survive in the absence of serum-specific growth factors. In addition, serum not only functions as a buffering agent but also offers protection against certain cytotoxic agents [10]. The choice of serum for the growth of hMSCs has a profound effect on the health and quality of the cells in culture, leading to a search for serum or suitable alternatives from other sources that display FBS-like properties but ideally are not of animal origin.

To overcome these issues, alternatives to FBS such as human platelet derivatives and human serum have been investigated. Platelets contain large amounts of growth factors and cytokines that are involved in the blood-clotting process, thus platelet lysate is rich in bioactive molecules. Recently, platelet lysate has been reported in the ex vivo expansion of hMSCs [11]. Human allogeneic serum (hAS) has been utilized previously for culturing telomerase-immortalized hMSCs and was found to be comparable to FBS [12].

In this study, hAS was used to compensate for the elimination of FBS in culture conditions optimized for human periosteum-derived cell (hPDC) expansion. Similar to hMSCs, hPDCs are multipotent stem cells that are able to differentiate along the adipogenic, chondrogenic, and osteogenic lineages. Despite their propensity for bone formation on calcium phosphate (CaP) scaffolds [13], little work has been done to create conditions for growth that would aid clinical translation of this cell population. To investigate the creation of a xeno-free, hPDC-containing combination product for bone tissue engineering applications, FBS was substituted for hAS during the expansion phase. Through the analysis of proliferation, lineage commitment, and signaling it was discovered that enhanced osteogenic differentiation and proliferation in vitro, in the presence of hAS, was associated with an improved tissue-forming capacity in vivo.

Materials and Methods

Collection of Human Allogeneic Serum

Human peripheral blood (20 ml) was collected from healthy volunteers (supplemental online Table 1) in BD vacutainer SST tubes (BD Biosciences, San Diego, CA, http://www.bdbiosciences.com). Subsequently, the blood was centrifuged at 1,000*g* for 10 minutes at room temperature, and the serum was collected and filtered through a 0.2-μm membrane (Millipore, Billerica, MA, http://www.millipore.com). All protocols were approved by the institutional review board of Leuven University, and written informed consent was obtained prior to sample collection. It was also ensured that no steroidal drugs or bisphosphonates had been taken by the volunteers in the past 12 months. Aliquots of sterile serum were stored at -20°C.

Culture of hPDC Populations

The hPDCs were maintained as described previously [14]. Details of cell populations can be found in supplemental online Table 1. All experiments were carried out with expanded cell populations between passages 5 and 7, with a seeding density of 4,500 cells per square centimeter. Cells were cultured in high-glucose Dulbecco's modified Eagle's medium (DMEM; Invitrogen, Carlsbad, CA, http://www.invitrogen.com) supplemented with 10% FBS (γ-Irradiated; Gibco, Grand Island, NY, http://www.invitrogen.com) or 10% hAS (collected as described previously) and antibiotic-antimycotic solution (100 U/ml penicillin, 100 μg/ml streptomycin, and 0.25 μg/ml amphotericin B; Invitrogen).

Analysis of In Vitro Cell Dynamics

Cell proliferation was determined through the measurement of DNA content of the cultures at defined time points during expansion in 10% FBS or hAS. Briefly, cell cultures were seeded at 1,000 cells per square centimeter and, following culture, harvested and lysed in 0.05% Triton X-100 ([Sigma-Aldrich, St. Louis, MO, http://www.sigmaaldrich.com] in phosphate buffered saline [PBS]). The DNA content was quantified using the Quant-iT dsDNA HS assay kit (Invitrogen). The concentration of DNA was converted to a predicted cell number using a predetermined value of 8.9 pg of DNA per hPDC [15]. Cell viability was characterized by staining the living and dead cells using the Live/Dead cell viability kit (Invitrogen). Alkaline phosphatase (ALP) levels were measured using the BluePhos Microwell Phosphatase Substrate System at 620 nm (Kirkegaard and Perry Laboratories Inc., Gaithersburg, Maryland, http://www.kpl.com). ALP activity was normalized to the DNA content of each well (R.U.: absorbance at 620 nm). To determine cell spreading, hPDCs were seeded in chamber slides before fixation in 4% formaldehyde. The actin cytoskeleton was visualized through staining with phalloidin conjugated to TRITC (Sigma-Aldrich, St. Louis, MO, http://www.sigmaaldrich.com), and nuclei were counterstained with 4′,6-diamidino-2-phenylindole. The cell-spreading ratio (length to width) was measured digitally using ImageJ software (National Institutes of Health, Bethesda, MD, http://rsb.info.nih.gov/ij/).

Analysis of hPDC Differentiation

To analyze the effect of hAS on hPDC differentiation into different lineages, cells were cultured for 14 days with 10% FBS or hAS, and gene expression of osteogenic, chondrogenic, adipogenic, or myogenic genes was measured. Total RNA was isolated using the RNeasy kit (Qiagen, Hilden, Germany, http://www.qiagen.com), and cDNA was synthesized with the SuperScript III First Strand synthesis system for real-time polymerase chain reaction (PCR; Invitrogen). Quantitative real-time SYBR Green (Invitrogen) PCR was performed according to the manufacturer's protocol, with mRNA levels normalized to β-actin expression. SYBR Green quantitative PCR (qPCR) primers were designed to span an intron so that only RNA-specific amplification was possible (primer sequences are shown in supplemental online Table 2). Total RNA samples subjected to cDNA synthesis reactions in the absence of reverse transcriptase were included as negative controls, and relative differences in expression were calculated using the $2^{-\Delta\Delta Ct}$ method [16].

Cell differentiation was further assessed through directed differentiation toward the osteogenic, chondrogenic, and adipogenic lineages. Briefly, to induce osteogenic differentiation, cells were seeded at 4,500 cells per square centimeter and allowed to proliferate for 48 hours before culture for 21 days in osteogenic medium (DMEM supplemented with 10% FBS or

hAS, 100 nM dexamethasone, 50 μg/ml ascorbic acid, and 10mM β-glycerophosphate). Differentiation was assessed through staining with alizarin red solution (pH 4.2). Quantification of calcium mineral deposits was performed by dissolving the dye with 10% cetylpyridinium chloride (in deionized water) for 60 minutes at room temperature. Absorbance was measured spectrophotometrically at 570 nm. Chondrogenic differentiation was assessed by culturing the cells in high-density micromasses (2×10^5 cells per 10 μl) in the presence of chondrogenic medium (DMEM Nutrient Mixture F-12, 2% serum, 1$\times$ insulin-transferrin-selenium-positive supplement, 100 nM dexamethasone, 10 μM Y27632, 50 μg/ml ascorbic acid, 40 μg/ml proline, and 10 ng/ml transforming growth factor β1) for 7 days. Differentiation was assessed with Alcian blue (proteoglycan) staining. Quantification of proteoglycans was carried out by extracting the Alcian blue dye from the micromass using 6M guanidine hydrochloride and measuring the absorbance at 620 nm. Adipogenic differentiation was assessed by seeding the cells at 1×10^4 cells per square centimeter followed by 14 days of culture in adipogenic induction media (α modification, minimum essential medium; 10% serum, 1 μM dexamethasone, 10 μg/ml human insulin, 100 μM indomethacin, and 25 μM IBMX). The efficiency of differentiation was assessed by Oil Red O staining followed by quantification of the lipid droplet area using ImageJ software (National Institutes of Health).

RT^2 Profiler PCR Array and Identification of Networks

In an attempt to elucidate the signaling molecules involved in human serum-directed osteogenic differentiation, the SABioscience (Qiagen) signal transduction pathway array was utilized. This qPCR array profiles the expression of 84 key genes representative of 18 different signal transduction pathways. The hPDCs were cultured for 14 days with 10% FBS or hAS, and total RNA was isolated using the RNeasy kit (Qiagen), as previously described. The single-strand cDNA from 1 μg total RNA was synthesized using the RT^2 first strand kit (Qiagen). Real-time PCR was performed according to the user manual of the RT^2 Profiler PCR array system (Qiagen) using SYBR Green PCR Master Mix in a StepOnePlus PCR system (Applied Biosystems, Foster City, CA, http://www.appliedbiosystems.com). Data analysis was carried out using the online SABioscience Array data analysis software, and genes were identified as up- or downregulated with a twofold or greater change in expression. Additional real-time PCR analyses were performed as previously described, with alternative primer sets for selected genes to validate the array data (supplemental online Table 2). Using the MIRna @Nd Transcription factor @nalysis Network site (MIR@NT@N), over-represented signaling pathways were identified through the KEGG database, and networks for more than twofold up- and downregulated genes were created.

Western Blotting of JAK-STAT-Associated Downstream Signaling Molecules

From the upregulated genes, JAK-STAT signaling was over-represented along with epithelial proliferation processes, therefore downstream signaling molecules involved in mediating mitogenic growth factor signal transduction were measured by Western blotting. For protein phosphorylation analysis, hPDCs were cultured for 14 days in 10% FBS or hAS, and lysates were prepared by adding lysis buffer containing protease and phosphatase inhibitors. Equal amounts of protein were loaded onto each lane of a 4%–12% Bis-Tris gel and subjected to electrophoresis under reducing conditions. After blotting, polyvinylidene difluoride membranes were blocked for 1 hour (5% milk powder in 0.1% PBS/Tween) and incubated with phosphoSTAT3 (pSTAT3) primary antibody (1:1,000), phospho-p44/42 MAPK (pERK) antibody (1:2,000), or phospho-CREB (pCREB) antibody (1:1,000; Cell Signaling Technology, Beverly, MA, http://www.cellsignal.com) overnight at 4°C. Binding of IgG horseradish peroxidase secondary antibody (1:2,000; DakoCytomation, Glostrup, Denmark, http://www.dakocytomation.com) was visualized by enhanced chemiluminescence. Normalization for total protein was performed by reprobing the membrane with mouse anti-mouse β-actin (1:1,000; Abcam, Cambridge, U.K., http://www.abcam.com) for 1 hour at room temperature, followed by goat anti-mouse IgG horseradish peroxidase (1:2,000; DakoCytomation) for 1 hour at room temperature.

Analysis of JAK-STAT3 in Response to hAS

The effect of JAK2 inhibition (JAK2 inhibitor [iJAK2] AG490 10 μM; Axon Medchem, Groningen, The Netherlands, http://www.axonmedchem.com/) and STAT3 inhibition (STAT3 inhibitor [iSTAT3] S3I-201 100 μM; Millipore) on the phosphorylation status of STAT3 in hPDCs was assessed by Western blot analysis. Briefly, cells were pretreated for 24 hours with each inhibitor before stimulation for 15 minutes with FBS or hAS. Western blots were carried out as described previously using pSTAT3 and total STAT3 (tSTAT3) antibodies at dilutions of 1:1,000. Quantification was carried out by band densitometry analysis, and pSTAT3 was normalized to tSTAT3 and β-actin. To assess the effect of this inhibition on proliferation, hPDCs were seeded at a density of 1,000 cells per square centimeter and cultured in 10% FBS or 10% hAS for periods of up to 6 days in the presence of each inhibitor. Media (including inhibitor) were refreshed every 2 days. Cell proliferation was assessed by DNA quantification (as described previously).

Analysis of In Vivo Bone Formation Following Human Serum Preconditioning

The hPDCs were cultured for 7 days in the presence of 10% FBS or hAS before being trypsin released, centrifuged, and resuspended at a concentration of 50 million cells per milliliter. Subsequently, 20 μl of the cell suspensions were applied to the upper surface of NuOss (Aceuropa, Lisbon, Portugal, http://www.aceuropa.com/) CaP scaffolds. To allow cell attachment, the seeded scaffolds were incubated overnight at 37°C. After incubation, the constructs were directly implanted subcutaneously in the back at the cervical region of NMRI-nu/nu mice. The remaining cells in the supernatant were counted to estimate the seeding efficiency, which was calculated as follows: [(number of seeded cells – number of cells in the supernatant) / number of seeded cells] $\times$ 100. After 56 days, the implants were collected and fixed in 4% formaldehyde before being scanned by high-resolution microfocus x-ray computed tomography (micro-CT). The explants were subsequently decalcified in ethylenediaminetetraacetic acid/PBS (pH 7.5) for 2 weeks before being paraffin embedded and processed for histology. All procedures on animal experiments were approved by the local ethical committee for animal research at KU Leuven. The animals were housed according to the guidelines of the Animalium Leuven at KU Leuven. To quantify ectopic bone formation, fluorescence histomorphometry, as described by Martin et al. [17], was performed on tissue sections from each implant. Briefly, fluorescent light microscopy images of sections stained with

hematoxylin and eosin (H&E) were acquired using a digital camera (model 25.4, Diagnostic Instruments Inc., Sterling Heights, MI, http://www.spotimaging.com/) on a Leica DMR microscope (Leica, Heerbrugg, Switzerland, http://www.leica.com). All images were taken at the same magnification (×25), size (1,600 × 1,200 pixels), file type (.tif) and brightness/γ settings. A measurement of the total tissue area and bone area in each fluorescent image was performed using an in-house developed MatLab (MathWorks, Natick, MA, http://www.mathworks.com) tool. The total tissue area was determined by an automatic threshold operation that picks out the scaffold perimeter from the dark background. Bone tissue was identified in the same images as areas that were brighter than a given threshold, which can be manually selected. In each case, the threshold was consistently applied to all images from an experimental set. The program subsequently calculated the percentage of bone that was present: (number of pixels contained in the bone area / number of pixels in the total area) × 100. Quantified images were generated by the program, which indicated the calculated scaffold area with a white line and the calculated bone area with a green line. These images were subsequently checked by the researcher for accurate identification of each structure.

Micro-CT Analysis of Explanted CaP/hPDC Constructs

Micro-CT was carried out on a Skyscan 1172 system (Skyscan NV, Kontich, Belgium, http://www.skyscan.be) at an isotropic voxel size of 4.5 μm^3. All explants were scanned using a source voltage and current of 60 kV and 167 μA, respectively, and a filter of 0.5 mm Al was applied. Using a rotation step of 0.3° over a total of 180° resulted in 640 radiographic images. After reconstruction using dedicated software, named NRecon (Skyscan), approximately 900 grayscale axial micro-CT images per sample were generated. Manual but consistent global segmentation of the CaP within each implant was carried out based on the grayscale histogram to allow quantification of parameters such as grain size distribution, surface area, and number of grains using commercially available image analysis software CTAn (Skyscan). The surface area of the CaP within the volume of interest (VOI) was measured three dimensionally using the marching cubes volume model (applied on the micro-CT voxel-based images) [16]. To analyze the composition of the newly formed bone, thresholds were determined to divide the in vivo-formed spicules into high-mineralized (HM) and low-mineralized (LM) fractions. The ratio of these fractions was calculated and indicates the overall composition of the formed tissue.

Histological Analysis

Histological staining was performed on paraffin-embedded sections of cell/biomaterial constructs. Briefly, paraffin sections were deparaffinized in Histo-Clear (Laborimpex, Brussels, Belgium, http://www.laborimpex.be/) and methanol and rinsed with distilled water. Sections were then stained for H&E, as described previously. In addition, Masson's trichrome staining was utilized to determine the abundance of mature bone and unmineralized cartilage, as described previously [18, 19].

RESULTS

Allogeneic Human Serum Increases hPDC Proliferation and Osteogenic Differentiation

To investigate the effect of allogeneic human serum on hPDC proliferation and viability, two different cell pools were cultured in the presence of three different pools of hAS (10%) and compared with FBS (10%). After 3 days, the appearance of cells grown in hAS differed from cells grown in FBS, with hAS-treated cells appearing smaller and less spread. After 6 days, the hAS-cultured cells had a more cuboidal morphology when compared with FBS-cultured cells (Fig. 1A). The hAS appeared to have no negative effect on cell viability (Fig. 1B); however, on analysis of cytoskeletal arrangement (Fig. 1C), the cells appeared smaller and less spread. Indeed, analysis of the width-length ratio revealed that hAS-cultured cells were approximately 1.8-fold ($p < .001$; $n = 3$) less spread than their FBS-cultured counterparts (Fig. 1E). Proliferation was significantly increased in all tested cell populations with all tested hAS pools, and similar growth curves were observed in each case (Fig. 1D). Cell number plateaued at day 10 (90,187 ± 5,819) and at this time was approximately 2.2-fold higher than FBS (40,974 ± 6,568). The number of cells was significantly higher ($p < .001$; $n = 3$) in all instances at all tested time points when compared with FBS. Endogenous ALP activity was 2.2-fold higher when cells were expanded in hAS ($p < .001$), indicating a potential osteogenic lineage commitment.

hPDCs Grown in Human Serum Display Increased Differentiation Toward the Osteogenic Lineage In Vitro

Following culture in 10% hAS for 14 days, the expression of osteoblast lineage markers RUNX2 and ALP were significantly increased by 1.6-fold and 2.8-fold, respectively ($p < .01$) (Fig. 2A, 2B). In addition, an increase in matrix mineralization of approximately 1.5-fold was observed following osteogenic differentiation in the presence of hAS when compared with FBS (Fig. 2C). Conversely, expression of chondrogenic differentiation markers SOX9 (Fig. 2D) and COL2A1 (Fig. 2E) displayed a trend for decreased expression, although this did not reach statistical significance (1.5-fold, $p = .173$; 2-fold, $p = .066$). Interestingly, an increase in chondrogenic differentiation was observed from hPDCs cultured in hAS, with a 1.25-fold increase in Alcian blue-positive proteoglycans present in this condition (Fig. 2F). As hPDCs have also been shown to possess the ability to differentiate into adipocytes and myoblasts [20], the expression of FABP4 and MyCH-2x was measured for adipogenic and myogenic lineage commitment, respectively. Human serum caused a 1.8-fold reduction in MyHC-2x expression, suggestive of an inhibition toward the myogenic lineage (Fig. 2G). Similarly, a 5.9-fold decrease in the expression of FABP4 was observed, suggesting that differentiation into adipocytes was significantly inhibited (Fig. 2H). Indeed, following directed adipogenic differentiation, a 6-fold reduction in Oil Red O-positive lipid area was observed when differentiation was carried out in the presence of hAS (1,150.5 ± 273.7 $\mu m^2/mm^2$ vs. 6,987.0 ± 1,090.6 $\mu m^2/mm^2$) (Fig. 2I).

Identification of Signal Transduction Factors Involved in Increased Proliferation and Osteogenic Differentiation With hAS

In order to identify the mechanisms involved in increased osteogenic differentiation with hAS expansion of hPDCs, cells were cultured in hAS or FBS for 14 days, RNA was extracted, and changes in gene expression of signal transduction factors were screened using the SABioscience signal transduction pathway array. From a possible 84 key genes representative of 18 different signal transduction pathways, 6 genes were upregulated by 2-fold or more

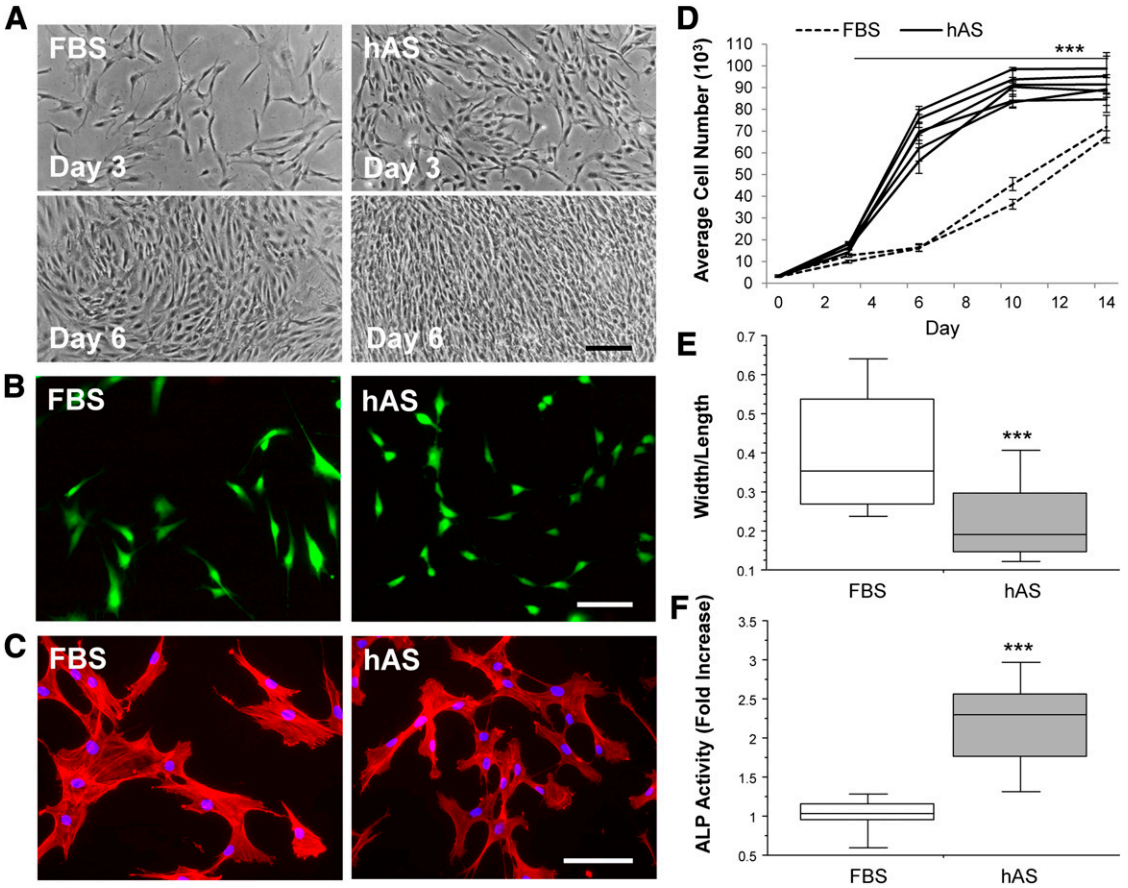

Figure 1. In vitro human periosteum-derived cell (hPDC) characteristics following culture in FBS or hAS. The hPDCs were cultured in 10% FBS or 10% hAS, as detailed in the Materials and Methods section. **(A):** Microscopic images depicting cellular morphology with FBS (left) or hAS (right) were taken at ×4 magnification following 3 days and 6 days of culture. **(B):** The viability of hPDCs is not affected through culture in hAS, as depicted by live/dead staining. Note the apparent absence of any dead (red) cells. **(C):** Cytoskeletal arrangement, as depicted by TRITC-phalloidin staining, is similar in both the FBS- and hAS-cultured cells; however, cell size is noticeably smaller in the hAS-cultured hPDCs. **(D):** Proliferation was robustly increased in all tested cell populations with all tested hAS pools, and similar growth curves were observed in each case. The number of cells was significantly higher ($p < .001$; $n = 3$) in all instances at all tested time points when compared with FBS. **(E):** When cell size was quantified, the ratio of width to length was significantly less in hAS-cultured hPDCs compared with FBS (1.8-fold; ***, $p < .001$; $n = 3$). **(F):** ALP activity was increased in hAS cultures (day 14) by 2.2-fold, which is indicative of osteogenic differentiation (***, $p < .001$; $n = 6$). Abbreviations: FBS, fetal bovine serum; hAS, human allogeneic serum.

and 16 were downregulated (Fig. 3A). Using alternative primers (supplemental online Table 2), qPCR analysis confirmed the trend for up- or downregulation of selected genes (supplemental online Fig.1). Using the MIR@NT@N gene expression network site, a number of downregulated genes could be linked to interferon-related pathways or protein kinase C signaling, creating IRF1-related and JUN-related networks (Fig. 3B). Although no networks were found for upregulated genes, JAK-STAT signaling and epithelial proliferation processes were over-represented (KEGG database and G-profiler, data not shown); therefore, downstream signaling molecules involved in mediating mitogenic growth factor signal transduction were measured by Western blotting. Phosphorylation of pSTAT3 protein was increased in hAS hPDCs compared with FBS, whereas phosphorylation of pERK and pCREB was decreased (Fig. 3C). Densitometry quantification of mitogenic signaling markers normalized to β-actin revealed a significant 36% increase in pSTAT3 phosphorylation, whereas the decrease in pERK (31%) and pCREB (92%) did not reach significance (Fig. 3D).

Inhibition of STAT3 Ablates hAS-Mediated Proliferation

In order to ascertain whether STAT3 is the main mediator of hAS-induced proliferation, cells were cultured in the presence of two inhibitors of the JAK-STAT pathway, iJAK2 (AG490; 10 μM) or iSTAT3 (S3I-201; 100 μM). As shown in Figure 4A, FBS-driven STAT3 phosphorylation was reduced by both iJAK2 and iSTAT3 (1.6-fold and 2.5-fold, respectively); however, in the case of hAS, only iSTAT3 reduced the phosphorylation of STAT3 (1.6-fold). FBS-mediated proliferation was inhibited by 98.2% (±0.23%) and 70.1% (±2.5%) when iSTAT3 and iJAK2 were administered to the cultures, respectively. In contrast, although iSTAT3 caused a decrease in hAS-mediated proliferation of 91.2% (±0.95%), inhibition of JAK2 only reduced proliferation by 12.1% (±5.94%) (Fig. 4B).

Bone Formation Is Increased In Vivo With hPDCs Precultured in hAS

To investigate the role of human serum culture conditions on in vivo bone formation, 1×10^6 hPDCs precultured for 7 days in

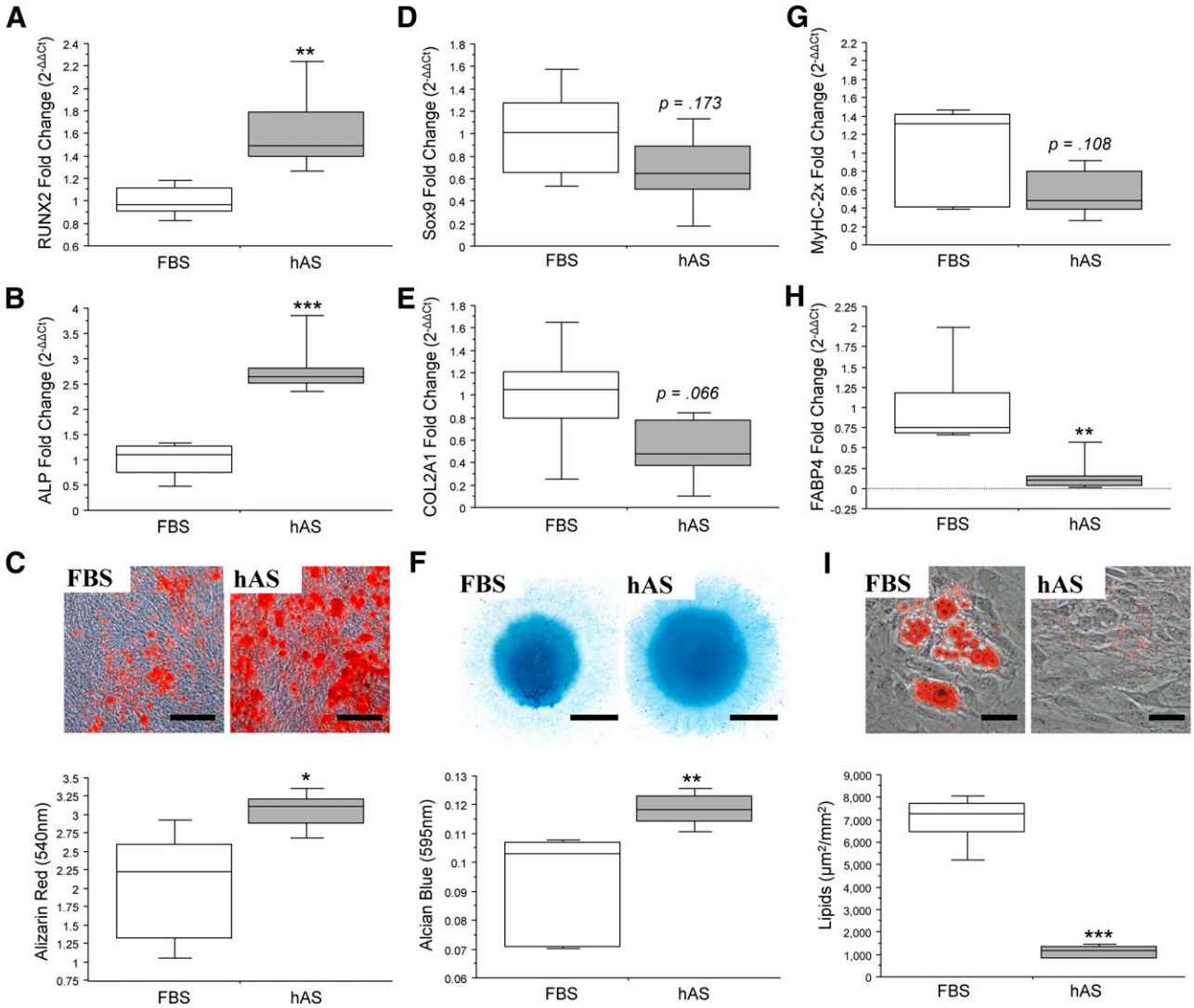

Figure 2. Effect of hAS on human periosteum-derived cell (hPDC) lineage commitment and differentiation. The hPDCs were cultured in 10% FBS or 10% hAS and analyzed for differentiation into osteogenic, chondrogenic, adipogenic, or myogenic lineages. Elevated expression of RUNX2 **(A)** and ALP **(B)** in hPDCs grown with hAS indicates increased commitment toward the osteogenic lineage. **(C):** On stimulation with osteogenic media a significant increase (***, $p < .05$; $n = 3$) in calcium phosphate deposition, as depicted by alizarin red staining, was observed (scale bar = 200 μm). A trend for decreased expression of Sox9 **(D)** and COL2A1 **(E)** was observed but not significant. **(F):** Micromass cultures of hPDCs undergoing chondrogenic differentiation in the presence of hAS showed a significantly higher quantity of glycosaminoglycan deposition than micromass cultures in FBS (scale bar = 2 mm; ***, $p < .01$; $n = 3$); however, the micromasses in hAS were larger in diameter. **(G):** Reduced expression of MyHC-2x suggested decreased myogenic commitment. **(H):** Similarly, a reduction in FABP4 expression suggested a decrease in hPDC commitment toward the adipogenic lineages that was confirmed by differentiating the cells in the presence of adipogenic media **(I)**. Large Oil Red O fat droplets are present in FBS-cultured cells but are small and dispersed in hAS cultured cells. On quantification, a significant 6-fold increase in fat droplet area was observed (scale bar = 50 μm; ***, $p < .001$; **, $p < .01$; $n = 3$). Abbreviations: FBS, fetal bovine serum; hAS, human allogeneic serum.

FBS or hAS were seeded onto 21-mm^3 NuOss scaffolds. No significant differences in cell-scaffold seeding efficiency were observed between the different serum types (FBS: 98.5% $\pm$ 0.57%; hAS: 96.75% $\pm$ 1.5%; $p = .07$). These cell-laden scaffolds were subsequently implanted subcutaneously in the back at the cervical region of NMRI-nu/nu mice for a period of 8 weeks. On explantation, histological examination revealed a clear increase in bone formation in scaffolds with hAS-precultured hPDCs. Analysis of H&E-stained sections also revealed the formation of bone marrow sinusoids in both FBS and hAS scaffolds (Fig. 5A, 5B). The volume of newly formed bone was quantified by histomorphometry (Fig. 5C) and revealed a significant increase in bone formation in hAS-precultured hPDC scaffolds compared with FBS (71% increase, $p < .001$).

hAS Culture Causes Alterations in Scaffold and Bone Matrix Composition

To determine whether culture in hAS has the ability to alter the dynamics of tissue formation, each explant was examined by micro-CT. Figure 6A shows representative micro-CT images (in grayscale and pseudocolor) of the explants, showing the contrast between bone (indicated by an asterisk or shown in orange) and

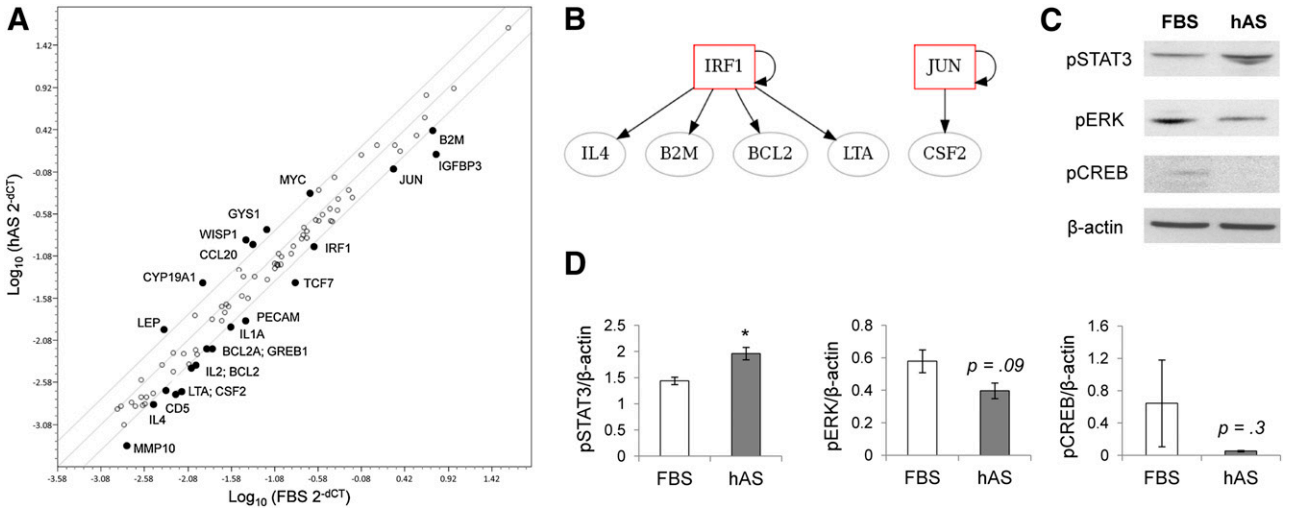

Figure 3. Alteration of signal transduction dynamics following culture in hAS. **(A):** Polymerase chain reaction array analysis of signal transduction factors revealed 6 upregulated, and 16 downregulated genes (2-fold or higher) in human periosteum-derived cells cultured in hAS for 14 days. **(B):** Using the MIRna @Nd Transcription factor @nalysis Network site (MIR@NT@N), no networks were found for upregulated genes; however, a number of downregulated genes could be linked to interferon-related pathways or protein kinase C signaling, creating IRF1-related and JUN-related networks. **(C):** From the upregulated genes, JAK-STAT signaling was overrepresented (G-profiler Kegg database, data not shown) along with epithelial proliferation processes; therefore, downstream signaling molecules involved in mediating mitogenic growth factor signal transduction were measured by Western blotting. Phosphorylation of pSTAT3 protein was increased in hAS hPDCs compared with FBS, whereas phosphorylation of pERK and pCREB was decreased. **(D):** Densitometry quantification of mitogenic mediators normalized to β-actin revealed a significant increase in pSTAT3 phosphorylation, whereas the decrease in pERK and pCREB did not reach significance ($*, p < .05$; $n = 3$). Abbreviations: FBS, fetal bovine serum; hAS, human allogeneic serum.

CaP grains (indicated by "g" or shown in blue). Furthermore, thresholds can be set for the CaP granules, and the granules can be segmented from the rest of the image. Interestingly, the increase in bone formation correlates to physicochemical changes in the CaP grains within the explants, where hAS treatment (dark gray) resulted in higher incidence of smaller grain sizes than FBS treatment (light gray) (Fig. 6B). This corresponds with a significantly lower surface area of CaP observed in the hAS-treated implants; however, the actual quantity of grains was not different between the two carriers (Fig. 6B). The presence of fibrous tissue (purple), CaP granules (blue/white), and mineralized tissue (green, HM; yellow, LM) was detected in both FBS- and hAS-scaffolds by micro-CT (Fig. 6C); however, the distribution of mineralization appeared different for each condition. To investigate this, thresholds were determined for both the LM and HM areas, and quantified. As shown in Figure 6C, a significant increase in LM to HM is observed when hPDCs are exposed to hAS in vitro. This finding was further investigated and validated through Masson's trichrome staining of FBS and hAS scaffold sections (Fig. 6D). Interestingly, NuOss scaffolds with hPDCs precultured in hAS displayed regions of immature osteoid (red staining), suggesting that the bone-formation process was still active within these constructs. Conversely, few regions of immature osteoid were present in the FBS-treated implants. The presence of immature (white) collagen fibrils within the hAS-treated implants was confirmed by polarized light microscopy (Fig. 6D).

Discussion

To allow the creation of a tissue-engineered implant that is able to recapture the fracture repair process, the progenitor population that normally mediates this process should be isolated and expanded. Much research has been directed on bone marrow MSCs as cells for bone engineering; however, when the specific role of bone marrow cells in fracture healing was investigated, it was found that although they contributed to the fracture callus, the cells were found exclusively surrounding the newly formed bone [21]. They have been hypothesized to be directly involved in modulation of the inflammatory response and formation of bone resorbing cells [22]. More recently, it has been demonstrated that although a proportion of osteoblasts originate from the bone marrow or endosteum, the major tissue involved in the production of local chondrocytes and osteoblasts during fracture repair is the periosteum [23]. To allow the realization of this cell source as a viable option for bone tissue engineering, we have reported extensively on their in vitro and in vivo capabilities [13, 14, 24–26], allowing for the formulation of a potential combination product for clinical translation [13]. In this study, we have described the expansion of periosteal progenitors (hPDCs) in hAS before implantation in an attempt to consider some of the challenges surrounding the translation of laboratory tissue engineering results from bench to bedside.

Although this study is the first to apply humanized culture conditions to hPDCs, a number of reports investigating the use of human serum with alternative stem cell populations have been published. Unfortunately, most of these studies contain conflicting data, indicating that the beneficial effects of using human serum may be cell specific [12, 27, 28]. Indeed, this was confirmed in part in a study by Nimura et al. (2008) where the specific effects of human serum on synovium and bone marrow-derived MSCs were investigated. Although an increase in proliferative capacity was observed in synovial MSCs when using human serum as compared with FBS, the opposite was true for bone marrow MSCs [27]. The authors concluded that this resulted from the differential

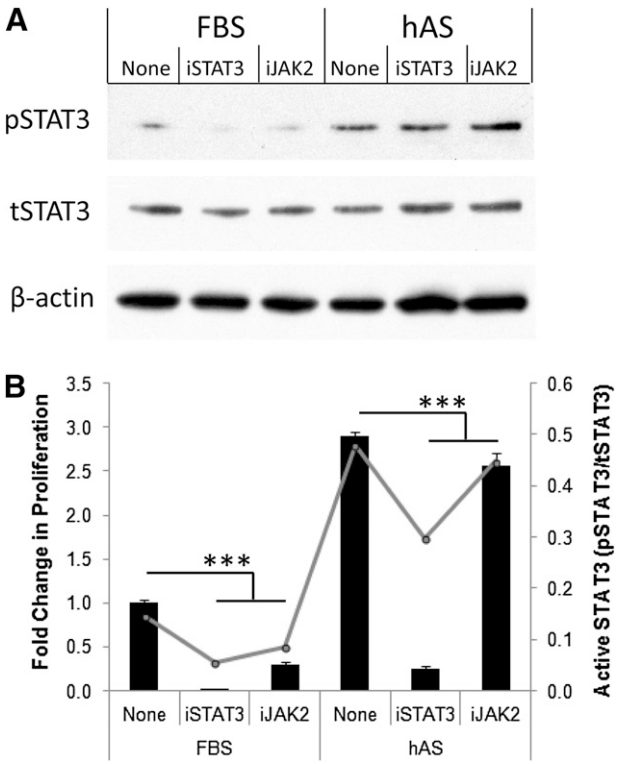

Figure 4. Effect of STAT3 inhibition on hAS-induced proliferation. Human periosteum-derived cells were cultured in 10% FBS or 10% hAS for periods of up to 6 days in the presence of iJAK2 (AG490; 10 μM) or iSTAT3 (S3I-201; 100 μM). **(A):** Western blot analysis of pSTAT3, following 15 minutes stimulation with FBS of hAS, showed that both iJAK2 and iSTAT3 caused a decrease in STAT3 phosphorylation when normalized to tSTAT3. **(B):** Proliferation (black bars) was significantly reduced in the presence of both inhibitors with both serums (***, $p < .001$; $n = 3$); however, the effect of iJAK2 on FBS-induced proliferation was 7-fold higher than that of hAS-induced proliferation. Densitometry quantification of pSTAT3 (gray line) normalized to β-actin and tSTAT3 correlated to the antiproliferative effect of the tested inhibitors. Abbreviations: FBS, fetal bovine serum; hAS, human allogeneic serum; iJAK2, JAK2 inhibitor; iSTAT3, STAT3 inhibitor; pSTAT3, phosphorylated STAT3; tSTAT3, total STAT3.

expression of the PDGFA receptor on the two cell types; however, specific effects of human serum on global signaling were not investigated. We also observed an increase in proliferative potential with a simultaneous change in cell size or spreading when culturing hPDCs in hAS. Interestingly, it has been shown previously that progenitor populations in bone marrow with a smaller size have higher self-renewal potential [29]. On analysis of signal transduction in the presence of hAS, it was found that the major downregulated network was related to interferon (IFN) signaling. It has been documented that IFNγ has a negative effect on in vitro osteogenic differentiation. Furthermore, T lymphocyte-produced IFNγ inhibits the bone-forming potential of bone marrow MSCs in vivo through the downregulation of Runx2 [30]. In addition, IFNγ has been shown to decrease the proliferative potential of human and mouse MSCs [31], thus the downregulation of this signal transduction pathway may contribute to the increased proliferation observed when hPDCs are cultured in hAS. Interestingly, FBS has previously been shown to enhance the activity of IFNγ; however, a comparison with human serum was not carried out, hence it is conceivable that this would also be the case for hAS [32]. Gene

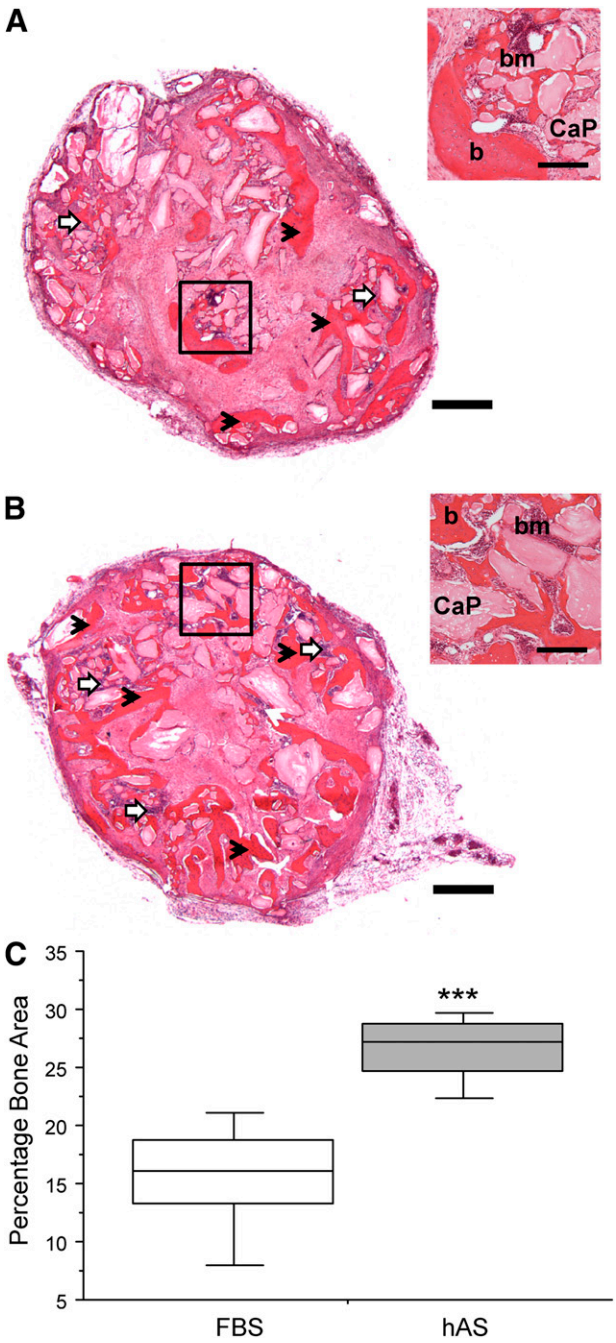

Figure 5. Bone formation in calcium phosphate scaffolds implanted in vivo with human periosteum-derived cells (hPDCs) precultured in FBS or hAS. Hematoxylin and eosin staining of scaffolds seeded with FBS-treated **(A)** or hAS-treated **(B)** hPDCs 8 weeks after implantation in NMRI-nu/nu mice. Bone spicules are indicated with black arrows and the presence of bone marrow by white arrows (scale bar = 500 μm). Insets highlight a magnified section of the scaffolds, where bone spicules, bone marrow, and calcium phosphate grains are highlighted (scale bar = 200 μm). **(C):** Quantification of histomorphometric images (20 per scaffold) for bone showed that hPDCs cultured in hAS before seeding initiated greater bone formation compared with hPDCs cultured in FBS ($n = 4$; duplicate implants in two mice per serum condition; ***, $p < .001$). Abbreviations: b, bone spicules; bm, bone marrow; CaP, calcium phosphate grains; FBS, fetal bovine serum; hAS, human allogeneic serum.

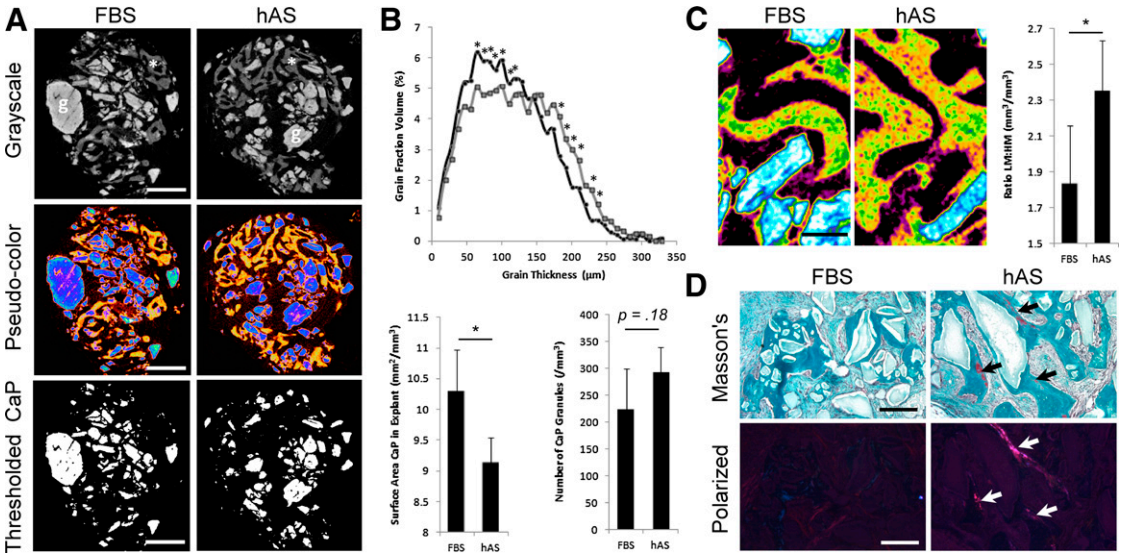

Figure 6. Postimplantation analysis of the scaffold and de novo formed bone. **(A):** Representative micro-CT images in grayscale and pseudo-colors, with thresholds for material associated CaPs (scale bar = 1 mm). **(B):** Analysis of CaP thickness distribution within the explants indicates a significant increase in smaller grain sizes with hAS-cultured human periosteum-derived cells (hPDCs) representative of increased resorption (∗, $p < .05$; $n = 3$). Comparison of the CaP surface area and the number of grains contained within the explants shows a significant decrease in surface area but not in number of grains when hPDCs are precultured with hAS (mean plus or minus standard deviation, $n = 3$). **(C):** Micro-CT images of explants seeded with FBS-treated or hAS-treated hPDCs (with gray to color translation), indicating CaP (white/blue) and mineralized tissue (green/orange-yellow) (scale bar = 200 μm). Note the apparent increase in low mineralized matrix (orange-yellow) compared with highly mineralized matrix (green). On quantification, the ratio of low mineralization to high mineralization was 1.3-fold higher in hAS-pretreated implants (∗, $p < .05$; $n = 3$). **(D):** The difference in matrix composition was confirmed by Masson's trichrome staining of FBS-treated or hAS-treated implants 8 weeks after implantation in NMRI-nu/nu mice. Areas of immature bone are stained red (indicated with arrows), whereas mature mineralized bone is stained blue (scale bar = 200 μm). Polarized light images (scale bar = 200 μm) verify the presence of immature (white) collagen fibrils within the hAS-treated implants. Note that the presence of immature bone may indicate that bone formation is still in an actively growing state within these scaffolds. Abbreviations: CaP, calcium phosphate grains; FBS, fetal bovine serum; hAS, human allogeneic serum.

ontology analysis indicated an over-representation of JAK-STAT signaling and epithelial proliferation processes from the upregulated genes, which, in combination with the increase in STAT3 phosphorylation observed, indicated the action of mitogenic growth factors. Inhibition of STAT3 phosphorylation modulated the proliferative action of hAS, whereas inhibition of JAK2 had little effect. This is in contrast with FBS-containing media, where inhibition of either JAK2 or STAT3 decreased cell proliferation by more than 90%. This finding indicates that JAK is not the main mediator of STAT3 phosphorylation in response to hAS. The kinases responsible for the phosphorylation of STAT3 appear to depend on the stimuli and the cell's environment [33]. It is hypothesized that the stimuli in this case may be interleukin 6, platelet-derived growth factor, or epidermal growth factor, or a combination of these, because it has been documented that these factors are present in serum and exert their effect on proliferation through the phosphorylation of STAT3. We have previously observed the positive mitogenic effect of epidermal growth factor on periosteal cell cultures [34].

As we have previously reported, hPDCs expanded in FBS are able to undergo robust bone tissue formation when implanted on CaP carriers [13, 35]. Consequently, it is important to define that this characteristic is not lost with the humanized culture conditions proposed in this study. It was found that the quantity and mineralization status of the de novo-formed bone was improved following transient culture in hAS. Furthermore, the dynamics of implant integration appeared altered, with a reduction in CaP granule size and surface area in the hAS condition when compared with FBS. This indicates an increase in CaP resorption by osteoclasts and may contribute to the increase in bone formation as osteoblast-osteoclast coupling is known to mediate the bone formation process [36]. In addition, it was observed that the bone spicules also contained a higher ratio of LM to HM matrix in hAS-precultured implants, indicating that the implant was continuing to grow, which was confirmed by the presence of newly formed osteoid. This may be explained by an increased proliferative or self-renewal potential of cells cultured in hAS when compared with FBS. Interestingly, hPDCs that were cultured in hAS display apparent altered lineage commitment with a decrease in the chondrogenic and adipogenic transcripts of Coll2a1 and FABP4, respectively, with a sequential increase in the osteogenic markers RunX2 and Coll1a1. This alteration in lineage commitment was partially confirmed through directed differentiation, where an increase in osteogenic differentiation and a decrease in adipogenic potential was observed in the presence of hAS. This has also been documented by Aldahmash et al., where reduction of the adipogenic marker PPARγ was observed following culture in hAS, although the authors stated nonsignificance of the data [12]. Interestingly, this same study reported no effect of hAS on proliferation, again, indicating cell specificity; however, the authors carried out the investigation using telomerase-immortalized cell clones. An increase in Coll1a1 expression has previously been documented in MSCs cultivated in human serum [28]. Although interesting, this is unlikely to be the main determinant causing the increase in bone formation; instead, the enhancement in cell proliferation is likely to play a greater role. MSC proliferation has previously been shown to be a key in vitro characteristic that could be correlated to in vivo bone forming capacity [37]. Moreover, culturing of slow proliferating cells in embryonic stem cell

media containing mitogenic growth factors rescued the bone-forming capacity of non-bone-forming populations.

Conclusion

We propose that the culture of hPDCs in hAS is a viable alternative to FBS for bone regenerative strategies, with positive mitogenic effects and skeletal lineage commitment associated with enhanced in vivo bone formation. Although the use of human-derived serum has obvious advantages when culturing populations in vitro for clinical translation, some considerations should be taken into account. It has been documented, for example, that age-related differences in serum composition occur and have a direct effect on MSC dynamics in vitro [38]; however, the data that is presented in this paper relates to pooled allogeneic serum from donors 23–81 years of age. Hence, it is likely that well-characterized pooled serum from healthy individuals would represent the most logical solution to this issue. With this in mind, the serum would have to be screened extensively to ensure that the risk of blood-borne pathogen transmission is at an absolute minimum.

Finally, and in view of our findings, the development of a clinical-grade hAS may be commercially attractive and have a use in MSC expansion and clinical translation of cellular therapies.

Acknowledgments

We thank Carla Geeroms and Kathleen Bosmans for excellent technical assistance. We also thank all collaborators of the Skeletal Biology and Engineering Research Center for useful comments and discussions. Funding for this research was obtained from the Stem Cell Institute of Leuven–KU Leuven and FW0 project 1508412N. S.J.R. is a postdoctoral fellow of the Research Foundation–Flanders (FWO). This work is also part of Prometheus, the Leuven Research and Development Division of Skeletal Tissue Engineering of the Katholieke Universiteit Leuven (http://www.kuleuven.be/prometheus).

Author Contributions

S.J.R. and H.C.O.: concept and design, collection and assembly of data, data analysis and interpretation, manuscript writing, final approval of manuscript; W.L.T.: collection and assembly of data, manuscript writing, final approval of manuscript; L.S.: collection and assembly of data, final approval of manuscript; S.J.V.C.: provision of study material or patients, final approval of manuscript; G.V.d.B.: financial support, provision of study material or patients, data analysis and interpretation, final approval of manuscript; F.P.L.: financial support, provision of study material or patients, data analysis and interpretation, final approval of manuscript.

Disclosure of Potential Conflicts of Interest

The authors indicate no potential conflicts of interest.

References

1 Caplan AI. Adult mesenchymal stem cells for tissue engineering versus regenerative medicine. J Cell Physiol 2007;213:341–347.

2 Jochems CE, van der Valk JB, Stafleu FR et al. The use of fetal bovine serum: Ethical or scientific problem? Altern Lab Anim 2002;30:219–227.

3 Erickson GA, Bolin SR, Landgraf JG. Viral contamination of fetal bovine serum used for tissue culture: Risks and concerns. Dev Biol Stand 1991;75:173–175.

4 Simonetti AB, Englert GE, Campos K et al. Nanobacteria-like particles: A threat to cell cultures. Braz J Microbiol 2007;38:153–158.

5 Horwitz EM, Gordon PL, Koo WK et al. Isolated allogeneic bone marrow-derived mesenchymal cells engraft and stimulate growth in children with osteogenesis imperfecta: Implications for cell therapy of bone. Proc Natl Acad Sci USA 2002;99:8932–8937.

6 Sundin M, Ringdén O, Sundberg B et al. No alloantibodies against mesenchymal stromal cells, but presence of anti-fetal calf serum antibodies, after transplantation in allogeneic hematopoietic stem cell recipients. Haematologica 2007;92:1208–1215.

7 van der Valk J, Mellor D, Brands R et al. The humane collection of fetal bovine serum and possibilities for serum-free cell and tissue culture. Toxicol In Vitro 2004;18:1–12.

8 Brunner D, Frank J, Appl H et al. Serum-free cell culture: The serum-free media interactive online database. ALTEX 2010;27:53–62.

9 Hodgson J. To treat or not to treat: That is the question for serum. Nat Biotechnol 1995;13:333–334.

10 Cifrian E, Guidry A, Marquardt WW. Role of milk fractions, serum, and divalent cations in protection of mammary epithelial cells of cows against damage by Staphylococcus aureus toxins. Am J Vet Res 1996;57:308–312.

11 Doucet C, Ernou I, Zhang Y et al. Platelet lysates promote mesenchymal stem cell expansion: A safety substitute for animal serum in cell-based therapy applications. J Cell Physiol 2005;205:228–236.

12 Aldahmash A, Haack-Sørensen M, Al-Nbaheen M et al. Human serum is as efficient as fetal bovine serum in supporting proliferation and differentiation of human multipotent stromal (mesenchymal) stem cells in vitro and in vivo. Stem Cell Rev 2011;7:860–868.

13 Roberts SJ, Geris L, Kerckhofs G et al. The combined bone forming capacity of human periosteal derived cells and calcium phosphates. Biomaterials 2011;32:4393–4405.

14 Roberts SJ, Chen Y, Moesen M et al. Enhancement of osteogenic gene expression for the differentiation of human periosteal derived cells. Stem Cell Res (Amst) 2011;7:137–144.

15 Zhou X, Holsbeeks I, Impens S et al. Non-invasive real-time monitoring by AlamarBlue® during in vitro culture of three-dimensional tissue-engineered bone constructs. Tissue Eng Part C Methods 2013;19:720–729.

16 Livak KJ, Schmittgen TD. Analysis of relative gene expression data using real-time quantitative PCR and the 2(-Delta Delta C(T)) Method. Methods 2001;25:402–408.

17 Martin I, Mastrogiacomo M, De Leo G et al. Fluorescence microscopy imaging of bone for automated histomorphometry. Tissue Eng 2002;8:847–852.

18 Hayami T, Pickarski M, Zhuo Y et al. Characterization of articular cartilage and subchondral bone changes in the rat anterior cruciate ligament transection and meniscectomized models of osteoarthritis. Bone 2006;38:234–243.

19 Chen L, Jiang W, Huang J et al. Insulin-like growth factor 2 (IGF-2) potentiates BMP-9-induced osteogenic differentiation and bone formation. J Bone Miner Res 2010;25:2447–2459.

20 De Bari C, Dell'Accio F, Vanlauwe J et al. Mesenchymal multipotency of adult human periosteal cells demonstrated by single-cell lineage analysis. Arthritis Rheum 2006;54:1209–1221.

21 Taguchi K, Ogawa R, Migita M et al. The role of bone marrow-derived cells in bone fracture repair in a green fluorescent protein chimeric mouse model. Biochem Biophys Res Commun 2005;331:31–36.

22 Colnot C, Huang S, Helms J. Analyzing the cellular contribution of bone marrow to fracture healing using bone marrow transplantation in mice. Biochem Biophys Res Commun 2006;350:557–561.

23 Colnot C. Skeletal cell fate decisions within periosteum and bone marrow during bone regeneration. J Bone Miner Res 2009;24:274–282.

24 Chai YC, Roberts SJ, Desmet E et al. Mechanisms of ectopic bone formation by human osteoprogenitor cells on CaP biomaterial carriers. Biomaterials 2012;33:3127–3142.

25 Chai YC, Roberts SJ, Schrooten J et al. Probing the osteoinductive effect of calcium phosphate by using an in vitro biomimetic model. Tissue Eng Part A 2011;17:1083–1097.

26 De Bari C, Dell'Accio F, Karystinou A et al. A biomarker-based mathematical model to predict bone-forming potency of human synovial

and periosteal mesenchymal stem cells. Arthritis Rheum 2008;58:240–250.

27 Nimura A, Muneta T, Koga H et al. Increased proliferation of human synovial mesenchymal stem cells with autologous human serum: Comparisons with bone marrow mesenchymal stem cells and with fetal bovine serum. Arthritis Rheum 2008;58:501–510.

28 Shahdadfar A, Frønsdal K, Haug T et al. In vitro expansion of human mesenchymal stem cells: Choice of serum is a determinant of cell proliferation, differentiation, gene expression, and transcriptome stability. STEM CELLS 2005; 23:1357–1366.

29 Haasters F, Prall WC, Anz D et al. Morphological and immunocytochemical characteristics indicate the yield of early progenitors and represent a quality control for human mesenchymal stem cell culturing. J Anat 2009;214:759–767.

30 Liu Y, Wang L, Kikuiri T et al. Mesenchymal stem cell-based tissue regeneration is governed by recipient T lymphocytes via IFN-γ and TNF-α. Nat Med 2011;17:1594–1601.

31 Croitoru-Lamoury J, Lamoury FM, Caristo M et al. Interferon-γ regulates the proliferation and differentiation of mesenchymal stem cells via activation of indoleamine 2,3 dioxygenase (IDO). PLoS ONE 2011;6:e14698.

32 Gao J, Folghera S, Fiorentini S et al. The influence of fetal calf serum on interferon-gamma induced HLA-DR expression on U937 cells. J Biol Regul Homeost Agents 1993;7: 115–120.

33 Ihle JN. STATs and MAPKs: Obligate or opportunistic partners in signaling. Bioessays 1996;18:95–98.

34 Eyckmans J, Roberts SJ, Bolander J et al. Mapping calcium phosphate activated gene networks as a strategy for targeted osteoinduction of human progenitors. Biomaterials 2013; 34:4612–4621.

35 Eyckmans J, Roberts SJ, Schrooten J et al. A clinically relevant model of osteoinduction: A process requiring calcium phosphate and BMP/Wnt signalling. J Cell Mol Med 2010;14 (6B):1845–1856.

36 Cao X. Targeting osteoclast-osteoblast communication. Nat Med 2011;17:1344–1346.

37 Janicki P, Boeuf S, Steck E et al. Prediction of in vivo bone forming potency of bone marrow-derived human mesenchymal stem cells. Eur Cell Mater 2011;21:488–507.

38 Abdallah BM, Haack-Sørensen M, Fink T et al. Inhibition of osteoblast differentiation but not adipocyte differentiation of mesenchymal stem cells by sera obtained from aged females. Bone 2006;39:181–188.

See www.StemCellsTM.com for supporting information available online.